The Plant Cell, Vol. 19: 1388–1402, April 2007, www.plantcell.org

Roles of *Arabidopsis* Cyclin-Dependent Kinase C Complexes in Cauliflower Mosaic Virus Infection, Plant Growth, and Development [W]

Xiaofeng Cui,[a] Baofang Fan,[a] James Scholz,[b] and Zhixiang Chen[a,1]

[a] Department of Botany and Plant Pathology, Purdue University, West Lafayette, Indiana 47907-2054
[b] Division of Plant Sciences, University of Missouri, Columbia, Missouri 65211

The C-terminal domain (CTD) of RNA polymerase II is phosphorylated during the transcription cycle by three cyclin-dependent kinases (CDKs): CDK7, CDK8, and CDK9. CDK9 and its interacting cyclin T partners belong to the positive transcription elongation factor b (P-TEFb) complexes, which phosphorylate the CTD to promote transcription elongation. We report that *Arabidopsis thaliana* CDK9-like proteins, CDKC;1 and CDKC;2, and their interacting cyclin T partners, CYCT1;4 and CYCT1;5, play important roles in infection with *Cauliflower mosaic virus* (CaMV). *cdkc;2* and *cyct1;5* knockout mutants are highly resistant and *cdkc;2 cyct1;5* double mutants are extremely resistant to CaMV. The mutants respond normally to other types of plant viruses that do not replicate by reverse transcription. Expression of a reporter gene driven by the CaMV *35S* promoter is markedly reduced in the *cdkc;2* and *cyct1;5* mutants, indicating that the kinase complexes are important for transcription from the viral promoter. Loss of function of *CDKC;1*/*CDKC;2* or *CYCT1;4*/*CYCT1;5* results in complete resistance to CaMV as well as altered leaf and flower growth, trichome development, and delayed flowering. These results establish *Arabidopsis* CDKC kinase complexes as important host targets of CaMV for transcriptional activation of viral genes and critical regulators of plant growth and development.

INTRODUCTION

The transcription of protein-coding genes in eukaryotes is performed by RNA polymerase II (RNAP II) and forms a so-called transcription cycle that includes preinitiation, initiation, promoter clearance, elongation, and termination (Sims et al., 2004). The transcription cycle starts with the assembly of the preinitiation complex at the promoter, which includes the general transcription factors TFIID, TFIIB, TFIIE, and TFIIH as well as RNAP II. Assembly of the preinitiation complex is followed by ATP-dependent melting of the double-stranded DNA (dsDNA) template and formation of an open complex between RNAP II and the DNA template. Once the open complex is established, transcription initiation occurs and RNAP II is allowed to clear the promoter and engaged to make the transition from initiation to elongation. Transcription elongation is a dynamic and highly regulated process that coordinates downstream events such as capping and splicing of primary transcripts. The final step in the cycle is transcription termination. At this stage, the mRNA is cleaved, polyadenylated, and transported to the cytoplasm for translation.

The transcription cycle involving RNAP II is accompanied by another cycling event: phosphorylation of the C-terminal domain (CTD) of the largest subunit of RNAP II (Sims et al., 2004). The RNAP II CTD contains multiple repeats of the heptapeptide sequence YSPTSPS (26 such repeats in yeast, 32 in *Caenorhabditis elegans*, 45 in *Drosophila*, and 52 in mammals). RNAP II in the preinitiation complex is unphosphorylated or hypophosphorylated, whereas transcription-competent RNAP II is heavily phosphorylated on its CTD, with Ser-2 and Ser-5 as the major modified residues. Phosphorylation of the CTD regulates the transition of RNAP II from initiation to elongation and the efficiency of elongation and pre-mRNA processing (capping, splicing, and polyadenylation).

Three cyclin-dependent kinases (CDKs), CDK7, CDK8, and CDK9, are involved directly in the phosphorylation of the CTD and in the regulation of different stages of the transcription cycle (Pinhero et al., 2004). CDK7 and its cyclin (Cyc) H partner are components of the general RNAP II transcription factor, TFIIH, involved in transcription initiation (Nigg, 1996). CDK8 and its CycC partner are also components of the RNAP II holoenzyme; they function to negatively regulate initiation by phosphorylation of the CTD of RNAP II and the CycH subunit of TFIIH (Akoulitchev et al., 2000). CDK9 and its CycT or CycK partner belong to the positive transcription elongation factor b (P-TEFb) (Marshall and Price, 1995).

In mammalian cells, several factors that function in elongation have been purified and identified, including P-TEFb, DSIF (for 5,6-dichloro-1-β-D-ribofuranosylbenzimidazole–sensitive-inducing factor), and NELF (negative elongation factor). Once transcription is initiated, NELF interacts with DSIF to induce RNAP II

[1] To whom correspondence should be addressed. E-mail zhixiang@purdue.edu; fax 765-494-5896.
The author responsible for distribution of materials integral to the findings presented in this article in accordance with the policy described in the Instructions for Authors (www.plantcell.org) is: Zhixiang Chen (zhixiang@purdue.edu).
[W] Online version contains Web-only data.
www.plantcell.org/cgi/doi/10.1105/tpc.107.051375

pausing, resulting in arrested transcription (Sims et al., 2004). P-TEFb can overcome the effects of the DSIF/NELF complex and release RNAP II from its arrest. P-TEFb phosphorylates the CTD of RNAP II, thus catalyzing the transition from initiation to elongation of transcription (Sims et al., 2004). In humans, P-TEFb is recruited by the Tat protein of human immunodeficiency virus type I (HIV-1) to stimulate transcriptional initiation and elongation (Mancebo et al., 1997).

Arabidopsis thaliana contains a single gene, *NRPB1* (At4g35800), encoding the largest subunit of RNAP II with a CTD containing 42 repeats of the YSPTSPS heptapeptide (Dietrich et al., 1990). CTD kinases and phosphatases that control the dynamic change of the CTD phosphoarray have also been identified in plants. In *Arabidopsis*, three genes encode D-type CDK7 proteins: CDKD;1, CDKD;2, and CDKD;3 (Shimotohno et al., 2003). CDKD;2 forms a stable complex with CycH;1 and exhibits high kinase activity toward the CTD of RNAP II. T-DNA insertion mutants for CDKD;1 and CDKD;3, however, exhibit no developmental defects throughout the life cycle under normal growth conditions, suggesting that the two CDK7 genes are not essential for plant development (Shimotohno et al., 2003). *Arabidopsis* contains a single gene encoding an E-type CDK8 protein (CDKE;1; At5g63610) with CTD kinase activity. CDKE;1, also known as HEN3, is required for the specification of stamen and carpel identities and for the proper termination of stem cells in the floral meristem (Wang and Chen, 2004). There are >20 genes encoding CTD phosphatase–like proteins (CPLs) in *Arabidopsis*, based on domain architecture identified in family member proteins of other eukaryotes (Koiwa et al., 2004). Genetic evidence indicates that CPL3 is a negative regulator of abiotic stress signaling (Koiwa et al., 2002). Thus, the dynamic regulation of CTD phosphorylation plays an important role in plant growth, development, and response to environmental conditions.

Proteins similar to C-type CDK9 have been reported in tomato (*Solanum lycopersicum*) (Joubes et al., 2001) and *Medicago* (Fulop et al., 2005). As with *CDK9* genes from other organisms, expression of these plant *CDK9* genes is not regulated by the cell cycle. Furthermore, the *Medicago* CDKC1/cyclin T1 kinase complex phosphorylates the CTD of RNAP II and restores the transcriptional activity of a HeLa nuclear extract depleted of endogenous CDK9 complexes (Fulop et al., 2005). Thus, plant CDK9/cyclin T complexes have a role in transcription similar to that of P-TEFb. *Arabidopsis* contains two genes encoding CDK9-like proteins, *CDKC;1* (At5g10270) and *CDKC;2* (At5g64960) (Menges et al., 2005), and five genes encoding cyclin T-like proteins, *CYCT1;1* (At1g35440), *CYCT1;2* (At4g19560), *CYCT1;3* (At1g27630), *CYCT1;4* (At4g19600), and *CYCT1;5* (At5g45190) (Wang et al., 2004). Yeast two-hybrid assays and in vitro immunoprecipitation have shown that both CDKC;1 and CDKC;2 interact with CYCT1;3, suggesting that they form P-TEFb–like complexes (Barroco et al., 2003). However, the biological roles of the *Arabidopsis* CDKC complexes have not been genetically analyzed.

In this study, we generated loss-of-function mutants for the two *CDKC* and five *CYCT1* genes from *Arabidopsis* for analysis of their roles in infection by *Cauliflower mosaic virus* (CaMV), a dsDNA virus that depends on host RNAP II for transcription. We also analyzed their phenotypes in leaf and flower growth, trichrome development, and flowering. Our results indicate that *Arabidopsis* P-TEFb–like kinase complexes are important host targets of CaMV for transcriptional activation of viral genes and critical regulators of plant growth and development.

RESULTS

Arabidopsis cdkc;2 and *cyct1;5* Mutants Are Resistant to CaMV

CaMV is a pararetrovirus whose DNA genome is replicated by the reverse transcription of an RNA intermediate. The CaMV genome consists of a circular dsDNA molecule of ~8 kb that forms a minichromosome in the nucleus of the host cell. It is transcribed unidirectionally by the cellular RNAP II into two major capped and polyadenylated transcripts, the *35S* and *19S* RNAs, from their own promoters (Hull, 2002). *Arabidopsis* is a host to CaMV; therefore, it can be used as a model system for the identification of host factors important for infection. Because of the reliance of CaMV on host RNAP II to synthesize its viral RNA templates for reverse transcription and translation, we examined the role in CaMV infection of *Arabidopsis CDKC;2*, which encodes a homolog to the CDK9 subunit of P-TEFb (Barroco et al., 2003) (see Supplemental Figure 1 online). We identified two independent T-DNA insertion mutants for *CDKC;2*: *cdkc;2-1*, with a T-DNA insertion in the 10th intron; and *cdkc;2-2*, with a T-DNA insertion in the 8th exon (see Supplemental Figure 2 online). RNA gel blotting failed to detect *CDKC;2* full-length transcripts of the expected size in either mutant. To determine the impact of the disruption of *CDKC;2* on CaMV infection, we mechanically inoculated wild-type and mutant plants with partially purified CaMV virons and compared them for disease symptom development. In wild-type plants, disease symptoms (initially vein clearing and chlorosis, followed by leaf stunting and curling) was first observed at ~10 to 12 d after inoculation (DAI); at 13 DAI, ~80% of wild-type plants had developed the symptoms (Figure 1A). At these stages, however, no disease symptoms were observed in the *cdkc;2* mutants (Figure 1A). At 15 DAI, 100% of wild-type plants but only 20% of the mutant plants developed disease symptoms (Figure 1A). During the remaining period up to 27 DAI, the percentages of the mutant plants that developed disease symptoms gradually increased and could reach up to 100% at 4 weeks after inoculation (Figure 1A). A similar delay in disease symptom development in the *cdkc;2* mutants was observed when the plants were inoculated by particle bombardment of an infectious CaMV DNA clone with artificial long terminal repeats (pCa122) (Kobayashi et al., 2002) (Figure 1B).

Accumulation of viral DNAs and RNAs was also examined in whole plants after inoculation by particle bombardment of pCa122. At 13 DAI, CaMV viral DNAs and RNAs were detected at high levels in wild-type plants but were undetected in the *cdkc;2* mutants (Figures 1C and 1D). At 17 DAI, viral DNAs were detected in the mutants, but their levels were substantially lower than those in the wild-type plants (Figure 1C). Likewise, reduced levels of viral RNAs were detected at 17 DAI in the *cdkc;2* mutants relative to those in the wild-type plants; the reduction was particularly pronounced for the full-length *35S*

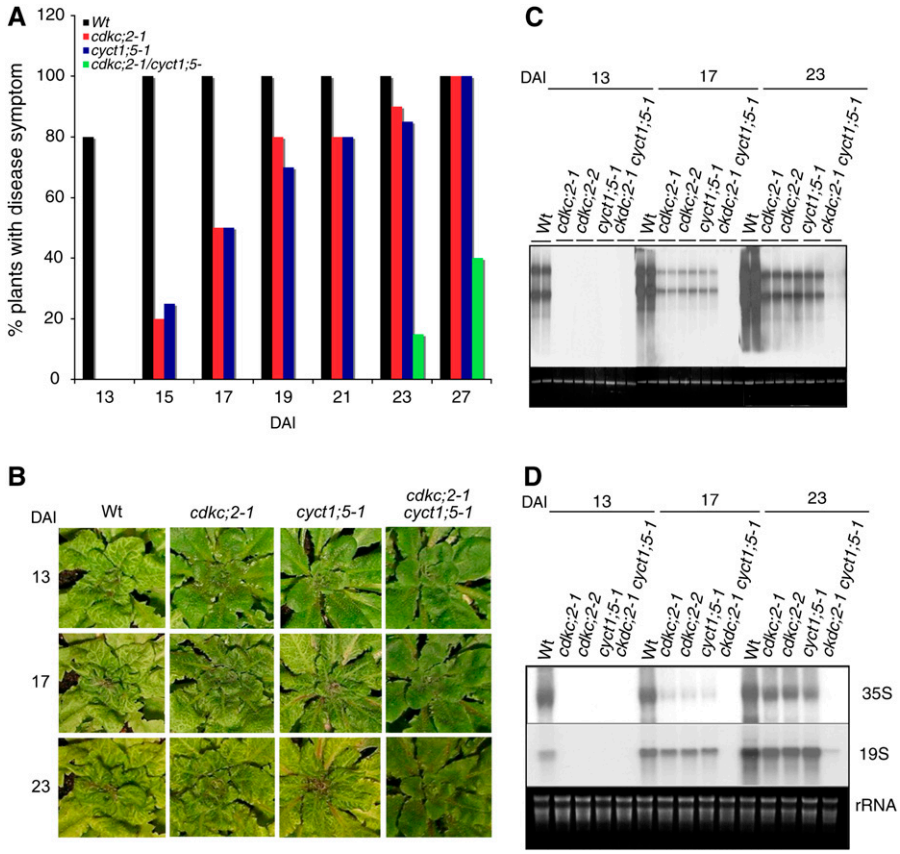

Figure 1. Enhanced Resistance of *cdkc;2* and *cyct1;5* Mutants to CaMV.

(A) Disease symptom development in mechanically inoculated plants. Forty wild-type, *cdkc;2-1*, and *cyct1;5-1* single or double mutant plants were mechanically inoculated with partially purified CaMV virons (0.5 mg protein/mL), and plants with CaMV mosaic symptoms were scored at the indicated DAI.
(B) Disease symptom development in plants inoculated by bombardment of the infectious CaMV DNA clone pCa122. Photographs of representative plants were taken at the indicated DAI. Disease symptom development in the *cdkc;2-2* mutant was the same as in the *cdkc;2-1* mutant.
(C) Viral DNA accumulation. Wild-type and mutant plants were inoculated by bombardment of pCa122, and total DNA was isolated from leaf tissues harvested at the indicated DAI and probed with the *P6* open reading frame of CaMV. Ethidium bromide staining of genomic DNA is shown as a loading control.
(D) Viral RNA accumulation. Total RNA was isolated from inoculated plants and first probed with the *P3* open reading frame of CaMV for detection of the *35S* RNA. The blot was stripped and reprobed with the *P6* open reading frame of CaMV for detection of the *19S* RNA. Ethidium bromide staining of rRNA is shown for the assessment of equal loading.

RNA (Figure 1D). At 23 DAI, the viral RNAs in the mutants increased to relatively high levels but were still substantially lower than those in the wild-type plants (Figure 1D). Thus, similar to disease symptom development, the accumulation of CaMV DNAs and RNAs was substantially delayed and reduced as a result of the disruption of the host *CDKC;2* gene.

The CDK9 subunit of P-TEFb forms functional kinase complexes with multiple cyclin T subunits (Peng et al., 1998). *Arabidopsis* contains five genes encoding cyclin T–like proteins (CYCT1;1 to CYCT1;5) (Wang et al., 2004). T-DNA insertion mutants were identified for *CYCT1;1* to *CYCT1;4* (see Supplemental Figure 2 online) from various collections, but they exhibited no altered phenotypes in response to CaMV infection. On the other hand, the *cyct1;5-1* T-DNA insertion mutant was deficient in its capacity to support CaMV infections, a phenotype strikingly similar to that of the *cdkc;2* mutants. As in the *cdckc;2* mutants, disease symptom development was delayed by 3 to 4 d in the *cyct1;5-1* mutant relative to that in wild-type plants after CaMV inoculation (Figures 1A and 1B). Accumulation of viral DNAs and RNAs was also similarly reduced in the *cyct1;5-1* mutant relative to that in wild-type plants (Figures 1C and 1D). To confirm that the altered response of the *cyct1;5-1* mutant to CaMV was due to the disruption of *CYCT1;5*, we performed genetic complementation of the mutant. A full-length *CYCT1;5* cDNA clone was placed behind its native promoter and transformed into the *cyct1;5-1* mutant. Transformants were identified through BASTA selection and analyzed for CaMV infection. Transformation of the mutant with *CYCT1;5* resulted in complete recovery of the wild-type phenotype in CaMV response (see Supplemental Figure 3 online). This finding indicates that the

enhanced resistance of the *cyct1;5-1* mutant to CaMV is the result of the disruption of *CYCT1;5*.

To determine whether the mutants for the two genes have additive effects on CaMV resistance, we generated *cdkc;2 cyct1;5* double mutants through genetic crosses. After CaMV infection, disease symptom development was further delayed in the double mutants compared with the *cdkc;2* and *cyct1;5* single mutants (Figures 1A and 1B). Thus, at ~3 weeks after CaMV inoculation, almost 100% of the *cdkc;2* and *cyct1;5* single mutants developed disease symptoms, but only10 to 20% of the *cdkc;2 cyct1;5* double mutant plants started to develop mild mosaic symptoms (Figures 1A and 1B). During the remaining period of the experiments, up to 4 weeks after inoculation, the percentage of the *cdkc;2 cyct1;5* double mutant plants exhibiting symptoms increased, but 40 to 50% of the mutants failed to develop any symptoms at all (Figure 1A). Accumulation of viral DNA and RNA was also further delayed and reduced in the double mutants compared with the single mutants. At 17 DAI, viral DNAs and RNAs were detected in *cdkc;2* and *cyct1;5* single mutants, albeit at reduced levels relative to those in wild-type plants; no viral DNAs or RNAs were detected in the *cdkc;2 cyct1;5* double mutants at this stage (Figures 1C and 1D). Even at the very late stages of infection (e.g., at 23 DAI), only trace amounts of viral DNAs and RNAs were detected in the *cdkc;2 cyct1;5* double mutants (Figures 1C and 1D). These results indicate that the *cdkc;2 cyct1;5* double mutants were extremely resistant to CaMV.

To determine whether the observed resistance of the *cdkc;2* and *cyct1;5* mutants to CaMV infection is specific to CaMV, we tested the mutants for their responses to a tobamovirus (tobacco mosaic virus isolate cg [TMV-cg], a RNA virus) (Ishikawa et al., 1991) and a geminivirus (*Cabbage leaf curl virus* [CaLCuV], a single-stranded DNA virus) (Turnage et al., 2002). After inoculation of three lower fully expanded leaves with purified TMV-cg virons, the *cdkc;2* and *cyct1;5* single and double mutants accumulated viral RNAs in both lower inoculated leaves and upper systemically infected leaves to levels similar to those in wild-type plants (Figure 2A). When infectious DNA clones of CaLCuV were inoculated through particle bombardment, these mutants also accumulated the same levels of viral DNAs as wild-type plants (Figure 2B). Thus, these mutants respond normally to TMV-cg and CaLCuV, two viruses that do not replicate through a reverse transcription mechanism.

Reduced CaMV *35S* Promoter Activity in the *cdck;2* and *cyct1;5* Mutants

The CaMV *35S* promoter, which directs the production of the *35S* pregenomic RNA, is strongly active in plant cells in the absence of any viral protein (Odell et al., 1985). To test whether CDKC;2 and CYCT1;5 are important for the viral promoter activity, we transformed the *cdkc;2* and *cyct1;5* mutant plants with a construct containing a β-glucuronidase (*GUS*) reporter gene driven by the CaMV *35S* promoter. As controls, the same reporter gene construct was also transformed into the wild type and the *cyct1;2-1* insertion mutant, which responds normally to CaMV (see Supplemental Figure 2 online). To determine the transgene expression, we assayed GUS activity and *GUS* transcripts in 15 to 20 independent wild-type or mutant transformants. In the wild-type background, the transformants had an average of ~265 units of GUS activity (Figure 3A) and accumulated high levels of *GUS* transcripts (Figure 3B). In the *cdkc;2* and *cyct1;5* single mutant backgrounds, the average GUS activities were ~65 units, representing a fourfold reduction from those in the wild-type plants (Figure 3A). The reduced GUS activity in these single mutant transformants was correlated with reduced levels of *GUS* transcripts (Figure 3B). In the *cdkc;2 cyct1;5* double mutant background, the average GUS activity was further reduced to ~35 units, and the reduced GUS activity was correlated with the very low levels of *GUS* transcripts in the double mutant transformants (Figure 3). By contrast, both the GUS activities and *GUS* transcripts in the *cyct1;2* mutant transformants were similar to those in the wild-type transformants (Figure 3). Thus, CDKC;2 and CYCT1;5 are required for the high CaMV *35S* promoter activity.

Complete CaMV Resistance of the Non-Null *cdkc;1 cdkc;2* and *cyct1;4 cyct1;5* Double Mutants

Although the *cdkc;2* and *cyct1;5* mutants are null, they behave like leaky mutants in that they are not completely resistant to CaMV and there is an additive effect between the two mutants in CaMV resistance (Figure 1). The leaky phenotypes of the null mutants are probably due to the presence of functionally related homologs. *Arabidopsis* CDKC;2 and CYCT1;5 are structurally closely related to CDKC1 and CYCT1;4, respectively (see Supplemental Figure 1 online). Because there is no knockout mutant for *CDKC;1* and the double knockout mutant of *cyct1;4*$^{-/-}$ and *cyct1;5*$^{-/-}$ is embryo-lethal (see below), we transformed a *CDKC;1* RNA interference (RNAi) construct into *cdkc;2-1* and a *CYCT1;4* RNAi construct into *cyct1;5-1* to generate non-null double mutants. T1 transgenic plants (*cdkc;2/CDKC;1 RNAi* and *cyct1;5/CYCT1;4 RNAi*) with suppressed expression of the targeted genes were identified by RT-PCR (see Supplemental Figure 4 online) and tested for CaMV resistance. The non-null *cdkc;2/CDKC;1 RNAi* and *cyct1;5/CYCT1;4 RNAi* double mutants as well as wild-type plants and *cdkc;2 cyct1;5* double knockout mutant plants were inoculated by bombardment with the infectious pCa122 CaMV DNA clone. At 18 DAI, viral DNAs and RNAs were observed in the wild type but not in any of the double mutants (Figure 4). At 26 and 35 DAI, however, significant levels of viral DNAs and RNAs were detected in the *cdkc;2 cyct1;5* double mutant plants but not in the transgenic *cdkc;2/CDKC;1 RNAi* or *cyct1;5/CYCT1;4 RNAi* plants (Figure 4). Thus, loss of function of the non-null *cdkc;2/CDKC;1 RNAi* and *cyct1;5/CYCT1;4 RNAi* double mutants was completely resistant to CaMV.

CDKC;1 and CDKC;2 Interact with Multiple Cyclins and Are CTD Kinases

Based on established interactions of CDK9 kinases with CYCT subunits and the strikingly similar phenotypes of the *cdkc* and *cyct1* mutants in CaMV resistance, it is likely that CDKC;1 and CDKC;2 form P-TEFb–like complexes with CYCT1;4 and CYCT1;5 in plant cells. We tested possible interactions between these proteins using yeast two-hybrid assays. From a previously reported yeast two-hybrid screen, CYCT1;3 is an interacting partner for both CDKC;1 and CDKC;2 (Barroco et al., 2003) and

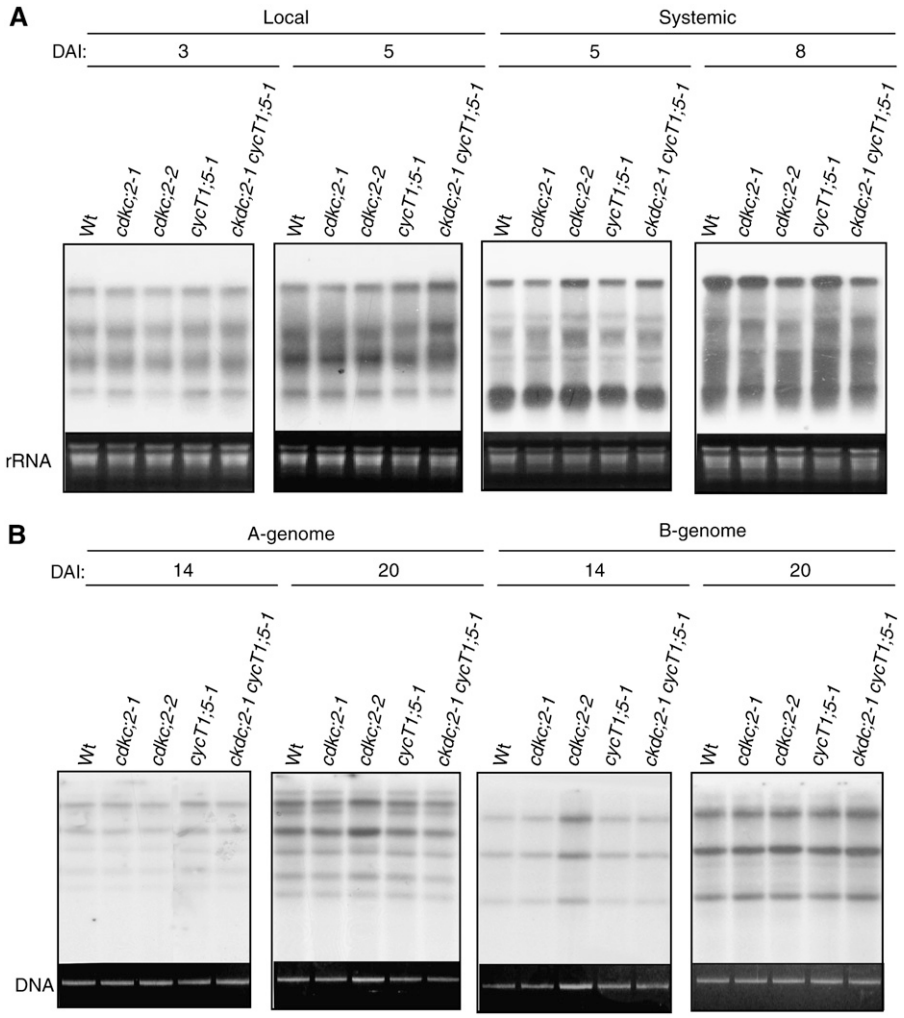

Figure 2. Response of *Arabidopsis cdkc;2* and *cyct1;5* Mutants to TMV-cg and CaLCuV.

(A) Accumulation of TMV-cg viral RNAs. Three leaves of 4-week-old *Arabidopsis* plants were inoculated with TMV-cg (5 μg/mL). The lower, inoculated leaves and upper, systemic infected leaves of five plants were collected at the indicated DAI for RNA isolation. RNA gel blot analysis was performed with ^{32}P-labeled TMV-cg coat protein gene as a probe.

(B) Accumulation of CaLCuV DNA-A and DNA-B. Four-week-old *Arabidopsis* plants were bombarded with the infectious DNA clones of CaLCuV. Total DNA was isolated from infected leaves at the indicated DAI. DNA gel blot analysis was performed with ^{32}P-labeled DNA fragments specific to the A or B components of CaLCuV.

was included in the assays as a positive control. We confirmed that both CDKC;1 and CDKC;2 interacted with CYCT1;3 but failed to detect their interactions with CYCT1;4 or CYCT1;5 in the yeast two-hybrid assays (Figure 5A).

To test whether *Arabidopsis* CDKC;1 and CDKC;2 are CTD kinases, we expressed their corresponding genes as well as *CYCT1;3* in *Escherichia coli* and purified their recombinant proteins. CYCT1;3 was chosen here because it interacts with CDKC;1 and CDKC;2 both in yeast and in vitro (Figure 5A) (Barroco et al., 2003). When assayed in the absence of CYCT1;3, the recombinant CDKC proteins were not able to phosphorylate the RNAP II heptapeptide (Figure 5B). When the recombinant CDKC proteins were assayed with CYCT1;3, phosphorylation of the heptapeptide was observed (Figure 5B). These results support the notion that *Arabidopsis* CDKC;1 and CDKC;2 are cyclin-dependent CTD kinases.

CDKC;1 and CDKC;2 might form P-TEFb–like kinase complexes with CYCT1;4 and CYCT1;5 in plant cells but not in yeast cells because formation of the complexes requires activation or accessory proteins not present in yeast cells. To test this, we examined their interactions in planta using the bimolecular fluorescence complementation (BiFC) assay (Walter et al., 2004) in *Agrobacterium tumefaciens*–infiltrated tobacco (*Nicotiana benthamiana*) leaves. CDKC;1 and CDKC;2 were fused to the N-terminal yellow fluorescent protein (YFP) fragment and CYCT1;4 and CYCT1;5 were fused to the C-terminal YFP fragment. CYCT1;3 interacts with CDKC;1 and CDKC;2 in yeast cells and was also fused to the C-terminal YFP fragment as a positive

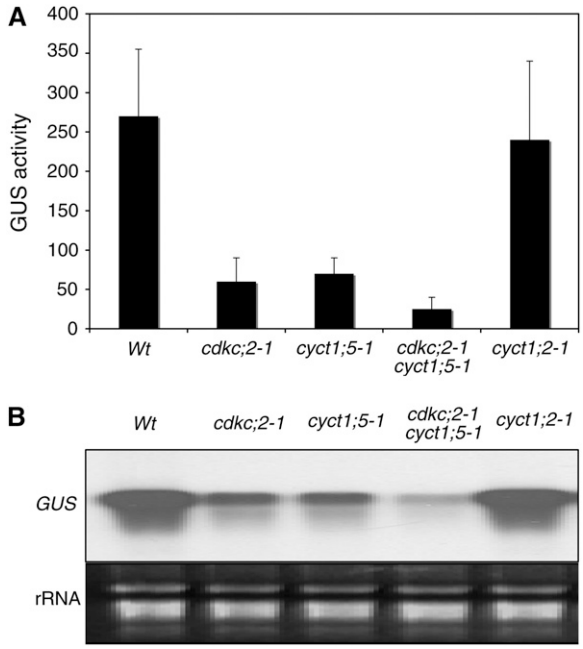

Figure 3. CDKC;2 and CYCT1;5 Dependence of the CaMV *35S* Promoter Activity.

(A) GUS activities in the wild type, *cdkc;2*, and *cyct1;5* mutants transformed with a *GUS* transgene driven by the CaMV *35S* promoter. Average GUS activities were calculated from 15 to 20 independent T1 transformants. GUS activities are expressed in units (nanomoles of 4-methylumbelliferone per minute per milligram of total soluble protein).
(B) Accumulation of *GUS* transcripts. Total RNA was pooled from 15 to 20 T1 transformants and probed with the full-length *GUS* gene fragment.

control. As expected, when the fused CDKC;1-N-YFP or CDKC;2-N-YFP was coexpressed with CYCT1;3-C-YFP in tobacco leaves, a strong BiFC signal was detected in the nuclear compartment of the transformed cells (Figures 5C and 5D). When the same CDKC;1-N-YFP or CDKC;2-N-YFP was coexpressed with CYCT1;4-C-YFP or CYCT1;5-C-YFP, a strong BiFC signal was also observed in the nuclear compartment (Figures 5C and 5D). Control experiments in which CDKC;1-N-YFP or CDKC;2-N-YFP was coexpressed with unfused C-YFP protein did not show any fluorescence (Figures 5C and 5D). These experiments provide strong evidence that CDKC;1 and CDKC;2 form complexes with CYCT1;4 and CYCT1;5 in plant cells.

Induced Expression of *CDKC* and *CYCT1* Genes by CaMV Infection

Because of their roles in CaMV infection, we analyzed the expression of these *CDKC* and *CYCT1* genes in CaMV-infected plants. Fully expanded lower leaves of 4-week-old *Arabidopsis* plants were mechanically inoculated with CaMV. As described above, it takes ~10 to 13 d after inoculation to first detect significant levels of CaMV viral DNA and observe symptom development in upper systemically infected leaves (Figure 1). As shown in Figure 6, the levels of transcripts for *CDKC;1*, *CDKC;2*, *CYCT1;4*, and *CYCT1;5* were quite constant during the first 10 DAI but increased substantially at 14, 18, and 24 DAI. Neither mock inoculation nor TMV-cg or CaLCuV inoculation induced expression of the genes (Figure 6). Thus, the four genes were induced specifically by CaMV infection.

Embryonically Lethal Null *cyct1;4 cyct1;5* Double Mutants

To test the functional redundancy of *CYCT1;4* and *CYCT1;5*, we initially attempted to generate *cyct1;4-1 cyct1;5-1* double

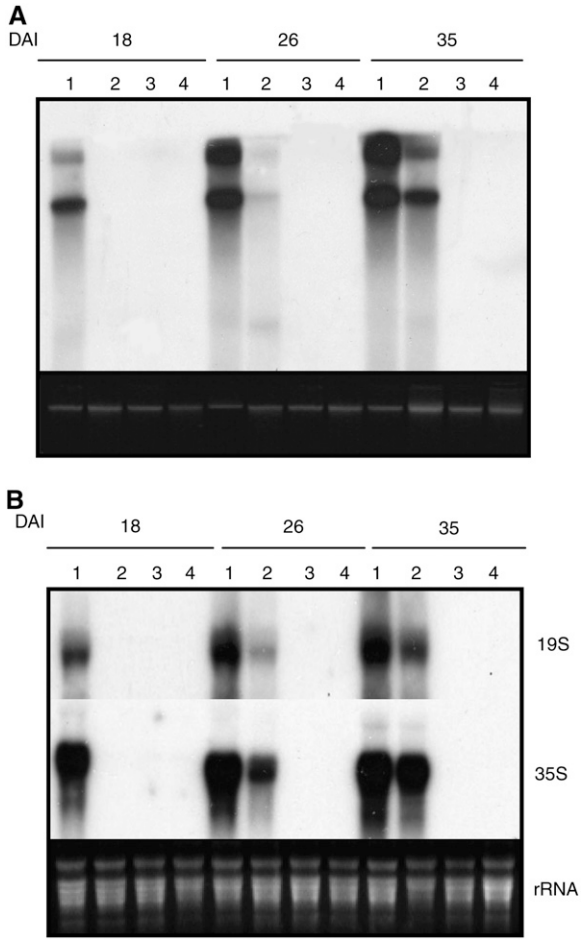

Figure 4. CaMV Resistance of the *cdkc;2/CDKC;1 RNAi* and *cyct1;5/CYCT1;4 RNAi* Mutants.

(A) Viral DNA accumulation. Wild-type (lane 1), *cdkc;2 cyct1;5* (lane 2), *cdkc;2/CDKC;1 RNAi* (lane 3), and *cyct1;5/CYCT1;4 RNAi* (lane 4) plants were inoculated by bombardment of pCa122, and total DNA was isolated from leaf tissues harvested at the indicated DAI and probed with the *P6* open reading frame of CaMV. Ethidium bromide staining of genomic DNA is shown as a loading control.
(B) Viral RNA accumulation. Total RNA was isolated from inoculated wild-type (lane 1), *cdkc;2 cyct1;5* (lane 2), *cdkc;2/CDKC;1 RNAi* (lane 3), and *cyct1;5/CYCT1;4 RNAi* (lane 4) plants. The RNA gel blot was first probed with the *P3* open reading frame of CaMV for detection of the *35S* RNA. The blot was stripped and reprobed with the *P6* open reading frame of CaMV for detection of the *19S* RNA. Ethidium bromide staining of rRNA is shown for the assessment of equal loading.

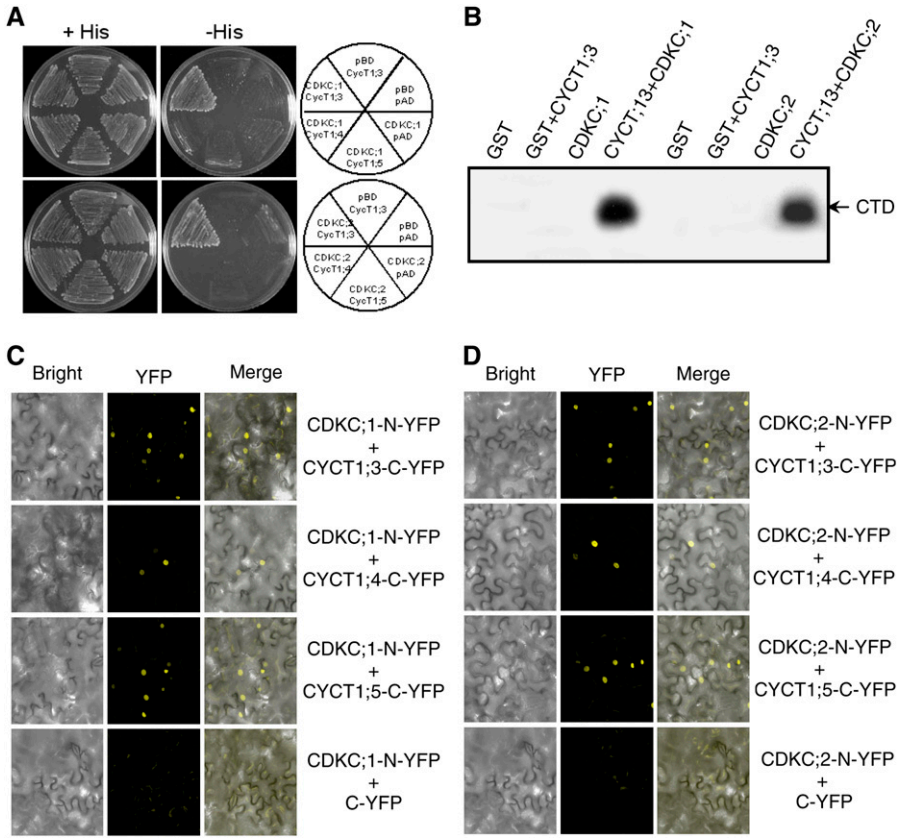

Figure 5. CDKC;1 and CDKC;2 Interact with CYCT1 Proteins and Phosphorylate the CTD Peptide.

(A) CDKC;1 and CDKC;2 interact with CYCT1;3 but not CYCT1;4 or CYCT1;5 in yeast cells. The Gal4 DNA binding domain–CDKC;1 or –CDKC;2 fusion vector was cotransformed with various activation domain–CYCT1 fusion vectors into yeast cells and grown in nonselective (+His) or selective (−His) medium. The empty DNA binding (pBD) and activation (pAD) vectors were included as negative controls. Growth without added His (−His) demonstrates interaction between protein pairs.

(B) Recombinant glutathione *S*-transferase (GST), GST-tagged CDKC;1 and CDKC;2, and His-tagged CYCT1;3 proteins were expressed and purified from *E. coli*. Phosphorylation of the GST-tagged CTD of RNAP II by the indicated proteins was assayed in the presence of [γ-^{32}P]ATP.

(C) and **(D)** BiFC analysis of CDKC;1 **(C)** and CDKC;2 **(D)** interactions in planta with CYCT1 proteins. Yellow fluorescence was observed in the nuclear compartment of *N. benthamiana* leaf epidermal cells, which results from complementation of the N-terminal part of the YFP fused with CDKC;2 (CDKC;2-N-YFP) with the C-terminal part of the YFP fused with CYCT1;3 (CYCT1;3-C-YFP) or CYCT;5 (CYCT1;5-YFP). No fluorescence was observed when CDKC;1-N-YFP or CDKC;2-N-YFP was coexpressed with unfused C-YFP. Bright-field images (left), YFP epifluorescence images (middle), and overlay images of plasmid autofluorescence and YFP epifluorescence (right) of the same cells are shown.

mutants through genetic crossing. About 120 F2 seedlings from *cyct1;4*$^{+/-}$ *cyct1;5*$^{+/-}$ F1 plants were genotyped by PCR but no *cyct1;4*$^{-/-}$ *cyct1;5*$^{-/-}$ homozygous double mutants were identified, although *cyct1;4*$^{+/-}$ *cyct1;5*$^{-/-}$ and *cyct1;4*$^{-/-}$ *cyct1;5*$^{+/-}$ plants were readily obtained. The absence of *cyct1;4*$^{-/-}$ *cyct1;5*$^{-/-}$ double homozygous mutants from the crosses could be the result of a gametophytic defect and/or a postfertilization, embryonic defect. To test possible gametophytic lethality, we conducted reciprocal crosses between wild-type and *cyct1;4*$^{-/-}$ *cyct1;5*$^{+/-}$ plants and genotyped the resultant F1 plants by PCR. As shown in Table 1, the F1 progeny from the reciprocal crosses comprised ~50% *cyct1;4*$^{+/-}$ *cyct1;5*$^{+/+}$ plants and 50% *cyct1;4*$^{+/-}$ *cyct1;5*$^{+/-}$ plants. We also conducted a genetic cross using a *cyct1;4*$^{+/-}$ *cyct1;5*$^{-/-}$ plant as the pollen donor and a *cyct1;4*$^{-/-}$ *cyct1;5*$^{+/-}$ plant as the pollen recipient. A total of 96 F1 progeny were analyzed and found to have a similar number of *cyct1;4*$^{+/-}$ *cyct1;5*$^{+/-}$, *cyct1;4*$^{-/-}$ *cyct1;5*$^{+/-}$, and *cyct1;4*$^{+/-}$/*cyct1;5*$^{-/-}$ plants (Table 1). These results indicate that double mutations of *cyct1;4* and *cyct1;5* can be cotransmitted through both types of gametophytes; therefore, failure to obtain *cyct1;4 cyct1;5* double homozygous mutants was due to zygote synthetic lethality. To confirm that the double homozygous mutations cause embryo lethality, we examined the seeds within the siliques of *cyct1;4*$^{-/-}$ *cyct1;5*$^{+/-}$ and *cyct1;4*$^{+/-}$ *cyct1;5*$^{-/-}$ plants. As shown in Figure 7A, ~25% of seeds from the siliques of both genotypes were aborted. The small, brown, aborted seeds and transparent embryos suggest that developmental arrest occurs during embryogenesis.

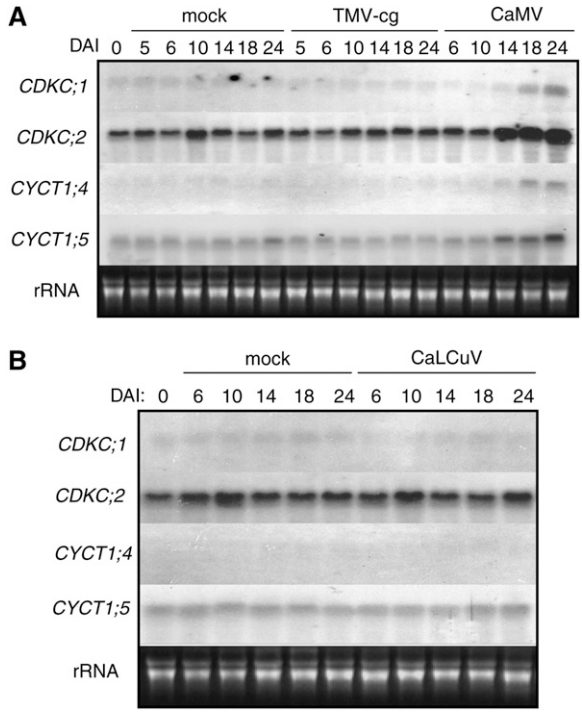

Figure 6. Induced Expression of *CDKC* and *CYCT1* Genes by CaMV.

Top, 4-week-old *Arabidopsis* plants were mechanically inoculated with TMV-cg or partially purified CaMV virions, with mock-inoculated (buffer only) plants used as controls. Bottom, plants were bombarded with the infectious DNA clones of CaLCuV or with gold particles (mock) as a control. Total RNA was isolated at the indicated DAI and probed with ^{32}P-labeled *CDKC* and *CYCT1* gene-specific DNA fragments.

Altered Growth and Development from Loss of Function of Both *CDKC;1* and *CDKC;2* or *CYCT1;4* and *CYCT1;5*

Both *cdkc;2/CDKC;1 RNAi* and *cyct1;5/CYCT1;4 RNAi* mutants showed clear differences in leaf development from the wild type (Figures 7B and 7C). The rosette leaves of the mutants were smaller and more curled and twisted than those of wild-type plants. The extent of the abnormal leaf growth of the mutant plants correlated with the degree of decrease of the transcripts for the targeted *CDKC;1* or *CYCT1;4* in the respective mutants (data not shown).

We examined *cyct1;5/CYCT1;4 RNAi* rosette leaves using scanning electron microscopy. A majority of adaxial trichomes of *cyct1;5/CYCT1;4 RNAi* leaves had two branches instead of the three branches found in typical trichomes of wild-type leaves. In addition, the adaxial surface of *cyct1;5/CYCT1;4 RNAi* leaves was rough and showed unusual cell and stomata shapes (Figure 7D)

Loss of function of the *CDKC* and *CYCT1* genes also resulted in delayed flowering. Compared with wild-type plants, flowering of the *cyct1;5* mutant was slightly but significantly delayed when grown under a medium (12-h) photoperiod (Figure 8A). The *cdkc;2* single mutants and the *cdkc;2 cyct1;5* double mutants, on the other hand, showed substantially delayed flowering and had increased numbers of rosette leaves at the time of bolting (Figure 8A). The most extensive delay in flowering, however, was observed in the non-null *cdkc;2/CDKC;1 RNAi* and *cyct1;5/CYCT1;4 RNAi* double mutants, which had almost twice as many rosette leaves as wild-type plants at the time of bolting under the growth conditions (Figure 8A).

The MADS box protein encoded by *FLOWERING LOCUS C* (*FLC*) functions as a repressor and is one of the central regulators of flowering in *Arabidopsis*. To examine the possible involvement of *FLC* in the delayed flowering of the mutants, we performed RNA gel blotting to compare mutant plants with wild-type plants for the levels of *FLC* transcripts. The *FLC* transcript was significantly elevated in the *cdkc;2*, *cdkc;2/CDKC;1 RNAi* and *cyct1;5/cyCYCT1;4 RNAi* mutants, which all displayed delayed flowering phenotypes (Figures 8A and 8B). The *FLC* transcript level was normal or slightly reduced in the *cyct1;5* single mutant, which exhibited only a slight delay in flowering. In the *cdkc;2 cyct1;5* double mutants, the *FLC* transcript level was only slightly higher than that in wild-type plants but substantially lower than that in the *cdkc;2* mutants, even though the double mutants flowered at least at late as the *cdkc;2* mutants (Figures 8A and 8B).

Functional Interaction of *CDKC;2* with *RNA-DEPENDENT POLYMERASE6* in the Regulation of Carpel Growth

P-TEFb has been shown to coordinate transcription with capping and 3′ end formation of primary transcripts (Ni et al., 2004; Adamson et al., 2005). Defects in capping and 3′ end formation were recently linked with *RNA-DEPENDENT POLYMERASE6* (*RDR6*)–mediated RNA silencing in *Arabidopsis* (Gazzani et al., 2004; Herr et al., 2006; Luo and Chen, 2007). These observations prompted us to examine possible functional interactions between CDKC and RDR6. We crossed *cdkc;2* with *rdr6-11* (Peragine et al., 2004) and found that double mutants exhibited similar phenotypes of slightly distorted rosette leaves and delayed flowering found in the parental *rdr6-11* and *cdkc;2* mutants (data not shown). However, unlike their parental single

Table 1. Genetic Analysis of the Lethal Phenotype of the *cyct1;4 cyct1;5* Double Mutant

Cross		Number of Plants					
Female	Male	Total	*cyct1;4*$^{+/-}$ *cyct1;5*$^{+/+}$	*cyct1;4*$^{+/-}$ *cyct1;5*$^{+/-}$	*cyct1;4*$^{-/-}$ *cyct1;5*$^{+/-}$	*cyct1;4*$^{+/-}$ *cyct1;5*$^{-/-}$	*cyct1;4*$^{-/-}$ *cyct1;5*$^{-/-}$
Wild type	*cyct1;4*$^{-/-}$ *cyct1;5*$^{+/-}$	40	19	21	0	0	0
cyct1;4$^{-/-}$ *cyct1;5*$^{+/-}$	Wild type	41	21	20	0	0	0
cyct1;4$^{-/-}$ *cyct1;5*$^{+/-}$	*cyct1;4*$^{+/-}$ *cyct1;5*$^{-/-}$	96	0	34	30	32	0

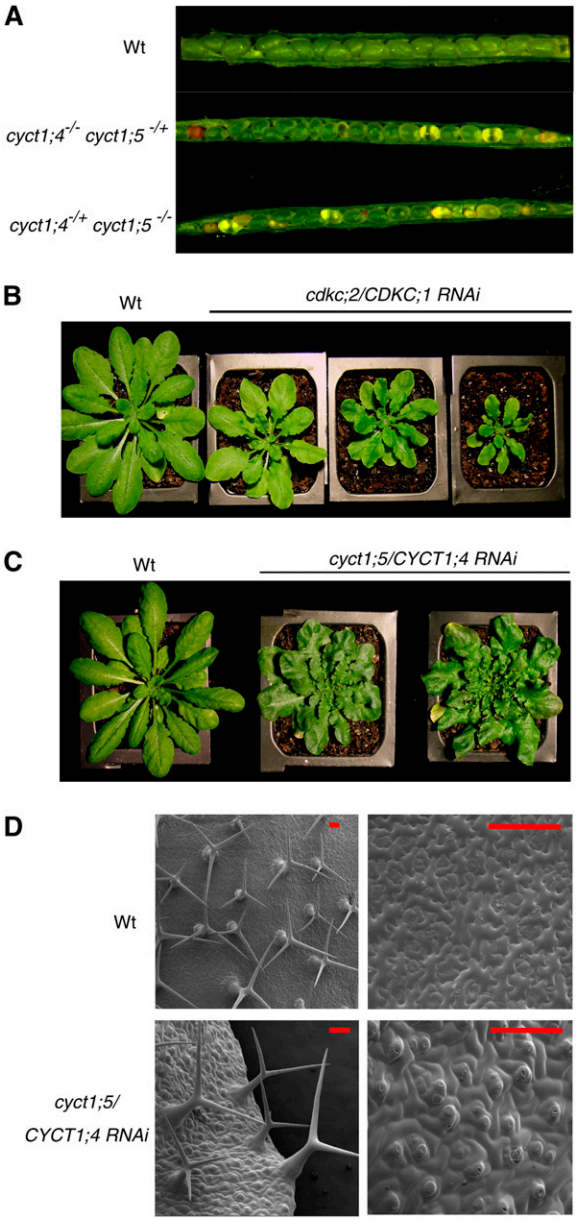

Figure 7. Growth Phenotypes of Double Mutants.

(A) Morphology of seeds from wild-type, *cyct1;4*$^{-/-}$ *cyct1;5*$^{-/+}$, and *cyct1;4*$^{-/+}$ *cyct1;5*$^{-/-}$ plants. The aborted seeds from siliques of mutant plants are either pale or brown and shrunken.

(B) Morphology of 6-week-old wild-type and transgenic *cdkc;2-1* mutant plants expressing a RNAi construct for *CDKC;1*. The extent of reduction in the size of the RNAi mutants was correlated with the extent of reduction in the level of *CDKC;1* transcripts, as determined by RT-PCR (data not shown).

(C) Morphology of wild-type and transgenic *cyct1;5* mutant plants expressing a RNAi construct for *CYCT1;4*. The altered leaf growth in the RNAi mutants was observed only in mutant plants with reduced levels of *CYCT1;4* transcripts, as determined by RT-PCR (data not shown).

(D) Scanning electron microscopy images of rosette leaf surfaces of wild-type and *cyct1;5/CYCT1;4 RNAi* mutant plants. Bars = 50 μm.

mutants, which set numbers of seeds similar to those of wild type when grown in normal conditions, the fertility of the *rdr6-11 cdk;2* double mutants was reduced by >80% (Figure 8C). The reduced fertility appeared to be a consequence of elongated carpels, such that pollen released from the anthers is unable to reach the stigma surface (Figure 8C). When manually fertilized, however, the double mutants could produce seeds, supporting our hypothesis that the mechanical defects in the coordinated growth of filaments and styles were mainly responsible for the drastically reduced fertility.

To explore the rather specific effect on carpel elongation associated with the disruption of *CDKC;2* in the *rdr6* mutant background, we examined possible tissue-specific expression of *CDKC;2* by analyzing the expression of a *GUS* reporter gene driven by the *CDKC;2* promoter in transgenic plants. For comparison, transgenic plants harboring the *GUS* reporter gene driven by the *CDKC;1* promoter were also generated and analyzed. In vegetative tissues, GUS expression was detected in all tissues, but the staining was particularly intense in the vascular veins of leaves for both *CDKC;1* and *CDKC;2* (data not shown). In flowers, we detected the highest *CDKC;2* expression in the carpels, particularly in the stigma and style (Figure 8D). By contrast, in flowers of transgenic plants expressing a *GUS* reporter gene driven by the *CDKC;1* promoter, the highest *GUS* activities were detected in stamens, particularly in anthers (Figure 8D).

DISCUSSION

Role of *Arabidopsis* CDKC Complexes in CaMV Infection

CaMV was the first plant virus to be found to contain DNA instead of RNA as genetic material (Shepherd et al., 1968, 1970) and has been studied extensively, particularly with regard to the roles of viral regulatory sequences and proteins involved in the transcription, replication, movement, and pathogenesis of the virus (Kiss-Laszlo and Hohn, 1996; Kobayashi et al., 2002; Stavolone et al., 2005). In addition, the CaMV *35S* promoter has been explored extensively for the expression of heterologous genes in transgenic plants. Despite this progress, little information is available about plant host factors targeted by the virus for the activation and regulation of transcription. Here, we report that *Arabidopsis* knockout mutants for *CDKC;2* and *CYCT1;5* are highly resistant to CaMV and the *cdkc;2 cyct1;5* double mutant is extremely resistant to CaMV (Figure 1). By contrast, these mutants respond normally to TMV-cg and CaLCuV (Figure 2). Expression of *Arabidopsis CDKC;2* and *CYCT1;5* is induced by infection with CaMV but not with TMV-cg or CaLCuV (Figure 6), and CDKC;2 can phosphorylate the CTD of RNAP II in the presence of an interacting cyclin subunit (Figure 5B). These results strongly suggest that the CDKC;2/CYCT1;5 complex functions as a P-TEFb and plays an important role in infection with CaMV.

There are two CDK9-like (*CDKC;1* and *CDKC;2*) and five CYCT1-like (*CYCT1;1* to *CYCT1;5*) genes in *Arabidopsis* (Barroco et al., 2003; Wang et al., 2004). When T-DNA insertion or Ds-tagged lines for these genes were analyzed for CaMV infection, only those for *CDKC;2* and *CYCT1;5* displayed enhanced resistance (Figure 1). These results suggest that CaMV utilizes

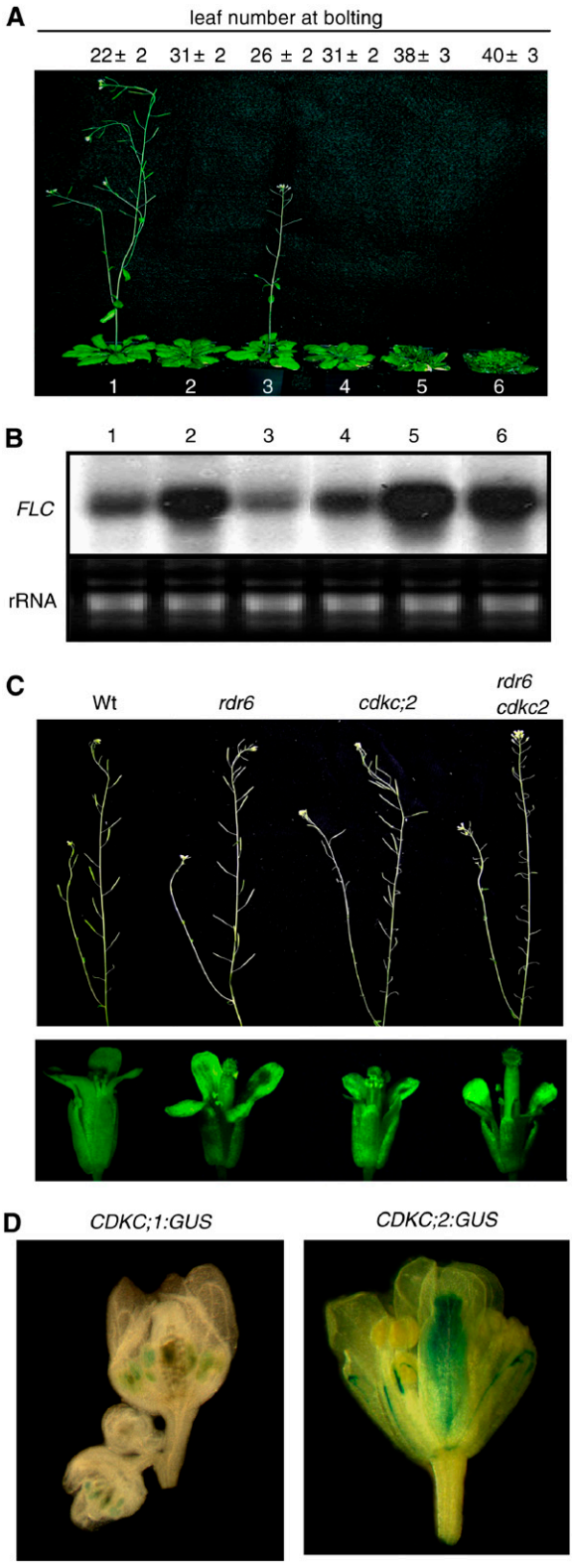

Figure 8. Phenotypes of Flowering and Flower Development of Double Mutants.

(A) Plants of the wild type (plant 1), *cdkc;2* (plant 2), *cyct1;5* (plant 3), *cdkc;2 cyct1;5* (plant 4), *cdkc;2/CDKC;1 RNAi* (plant 5), and *cyct1;5/CYCT1;4 RNAi* (plant 6) mutants grown under a 12-h-light/12-h-dark photoperiod. The photograph was taken 8 weeks after germination.

(B) *FLC* transcripts in 5-week-old plants of the wild type (lane 1), *cdkc;2* (lane 2), *cyct1;5* (lane 3), *cdkc;2 cyct1;5* (lane 4), *cdkc;2/CDKC;1 RNAi* (lane 5), and *cyct1;5/CYCT1;4 RNAi* (lane 6) mutants grown under a 12-h-light/12-h-dark photoperiod.

(C) Siliques (top panel) and flower buds (bottom panel) of wild-type, *rdr6-11*, *cdkc;2-1*, and *rdr6 cdkc;2* mutant plants.

(D) GUS activities in flower buds of stably transgenic *Arabidopsis* plants expressing *CDKC;1:GUS* (left) or *CDKC;2:GUS* (right). These images are representative results of multiple flowers buds examined from five independent transgenic lines for each construct.

specific members of these small protein families for the activation of transcription. However, although the *cdkc;2* and *cyct1;5* mutants are null based on the absence of their respective transcripts, they exhibited a leaky phenotype in that they were not completely resistant to CaMV (Figure 1). The leaky phenotypes are due to partial functional redundancy of the related CDKC and CYCT1 proteins. When the expression of *CDKC;1* and *CYCT1;4* was inhibited by RNAi in the respective *cdkc;2* and *cyct1;5* mutant backgrounds, we observed complete resistance to CaMV in the resultant non-null double mutants (Figure 4). Thus, CaMV may utilize preferentially, but not exclusively, CDKC;2 and CYCT1;5 for transcription activation. A high but not absolute specificity of targeting of similar host factors by CaMV might have advantages for the virus. Although the *cdkc;2* and *cyct1;5* mutants have largely normal growth and development, the *cyct1;4 cyct1;5* double mutant had a lethal phenotype. CaMV may have evolved to exploit the functional redundancy of these closely related proteins by preferentially targeting some of these transcription factors to avoid competition with the transcription of host genes, thereby reducing or avoiding a selection pressure from the host. On the other hand, different members of a gene family often exhibit differential cell- or tissue-specific expression patterns. If the targeting specificity were too stringent, CaMV transcription would be blocked in certain cells or tissues where genes encoding targeted factors are not expressed or are expressed at very low levels. An extremely high specificity would also limit the host range of the virus if the host factors required for viral transcription differed significantly in their structures, even among closely related plant species.

P-TEFb as an Evolutionarily Conserved Target of Retroviruses and Pararetroviruses

In humans, P-TEFb is targeted by HIV-1 and is required for its transcription and replication (Mancebo et al., 1997). A recent study reported that human T-lymphotropic virus type I, another complex retrovirus, recruits P-TEFb to stimulate viral gene transcription (Zhou et al., 2006). No such close link of P-TEFb has been reported with other animal DNA viruses (such as adenoviruses and herpes viruses) that also depend on host RNAP II for transcription (Flint and Shenk, 1997). Likewise, the *Arabidopsis cdkc;2* and *cyct1;5* mutants are resistant to CaMV (Figure 1) but respond normally to CaLCuV (Figure 2), DNA geminiviruses whose genes are also transcribed by host RNAP II

(Hanley-Bowdoin et al., 2000). Thus, P-TEFb appears to be an evolutionally conserved target of complex retroviruses and pararetroviruses for transcription activation. This remarkable conservation most likely reflects a fundamental mechanism unique to the transcription of these viruses.

Although human P-TEFb is not known to play a critical role in the transcription of any human DNA virus, its overexpression in human cells can greatly activate the in vivo activity of the cytomegalovirus promoter (Peng et al., 1998). Thus, P-TEFb has an ability to enhance the activity of promoters from other DNA viruses; therefore, it is intriguing that no animal DNA virus is known to recruit this host factor for transcription activation. Unlike retroviruses and pararetroviruses, the products of transcription of most DNA viruses are used primarily as templates for translation; therefore, these viruses can utilize not only transcriptional mechanisms but also a number of posttranscriptional mechanisms that mediate RNA splicing or RNA stability to maximize the production of viral gene products. In retroviruses and pararetroviruses, the full-length genomic or pregenomic RNA is multifunctional; it is utilized as a template for translation and as a template for genome replication through reverse transcription (Kiss-Laszlo and Hohn, 1996). This RNA must be stringently regulated to achieve the appropriate balance for translation or replication. While posttranscriptional mechanisms such as splicing are necessary for gene expression of retroviruses and pararetroviruses, they would be counterproductive for replication of the virus by depleting the full-length viral RNA templates required for reverse transcription. As a result, retroviruses and pararetroviruses may have to rely more on transcriptional mechanisms, such as those mediated by P-TEFb, to enhance the production of genomic or pregenomic RNA.

The long terminal repeat of HIV-1 has minimal promoter activity in the absence of the viral Tat protein (Brady and Kashanchi, 2005). The CaMV *35S* promoter, on the other hand, is strongly active in plant cells in the absence of any viral protein (Odell et al., 1985). By analyzing the expression of a reporter gene driven by the CaMV *35S* promoter, we have shown that CDKC;2 and CYCT1;5 are required for the high CaMV *35S* promoter activity (Figure 3). Thus, the CDKC;2/CYCT1;5 kinase complex might be recruited directly to the viral promoter for transcription activation. Since neither CDKC;2 nor CYCT1;5 is known to bind DNA, their recruitment by the *35S* promoter is probably mediated by cellular DNA binding transcription factors that recognize regulatory *cis*-acting DNA sequences in the CaMV *35S* promoter. It should also be pointed out that although the CaMV *35S* promoter alone can direct the synthesis of full-length transcripts from heterologous transgenes in transgenic plants, additional viral factors may be required for efficient synthesis of the much longer *35S* RNA during CaMV infection. These unidentified viral factors could function as additional recruiters of the cellular CDKC/CYCT1 complex to stimulate transcription, particularly transcription elongation.

Role of *Arabidopsis* CDKC Complexes in Plant Growth and Development

Although highly resistant to CaMV, the *cdkc;2*, *cyct1;5*, and *cdkc;2 cyct1;5* mutants exhibit largely normal growth and development. The relatively mild phenotypes of the mutants in plant growth and development were apparently due to the presence of functionally redundant homologs. CYCT1;5 is structurally most closely related to CYCT1;4, and the *cyct1;4 cyct1;5* double mutant was embryo-lethal (Table 1, Figure 7A), indicating that they are essential for plant growth. Based on the severe phenotypes of the non-null *cdkc;2/CDKC;1 RNAi* mutants, the two CDKC kinases most likely have overlapping, essential roles as well. Both the *cdkc;2/CDKC;1 RNAi* and *cyct1;5/CYCT1;4 RNAi* double mutants had altered leaf and trichrome growth compared with wild-type plants (Figure 7). The mutants also flowered late (Figure 8A) and produced drastically reduced numbers of seeds (data not shown). These results indicate that the CDKC complexes have important roles in both plant growth and development.

The most notable phenotype of the *cdkc;2* mutants was significantly delayed flowering (Figure 8A). Flowering was further delayed in the *cdkc;2/CDKC;1 RNAi* and *cyct1;5/CYCT1;4 RNAi* double mutants (Figure 8A). Delayed flowering of the mutants was associated with enhanced levels of *FLC* transcripts (Figure 8B). In *Arabidopsis*, early flowering and repression of *FLC* are observed in the mutants for *VIP4*, *ELF7*, and *ELF8* that encode homologs for subunits of PAF, a yeast transcription elongation complex containing Paf1, Cdc73, Ctr9, Rtf1, and Leo1 (Zhang and van Nocker, 2002; He et al., 2004; Oh et al., 2004). In yeast, PAF is linked to histone 3 Lys-4 methylation by the Set1 methyltransferase in actively transcribed genes (Krogan et al., 2003). ELF7 and ELF8 (homologs of Paf1 and Ctr9, respectively) are required for the enhancement of histone 3 Lys-4 methylation in *FLC* chromatin (He et al., 2004). More recent studies have revealed that the association of PAF with RNAP II is mediated by DISF, a transcription elongation factor known to interact both physically and functionally with P-TEFb (Qiu et al., 2006). Therefore, the observed regulation of *Arabidopsis* flowering time and *FLC* expression by genes encoding subunits of PAF and P-TEFb may be mechanistically linked. Intriguingly, while mutations of genes encoding subunits of PAF cause repression of *FLC* and early flowering (Zhang and van Nocker, 2002; He et al., 2004; Oh et al., 2004), mutations of genes encoding subunits of P-TEFb lead to elevated levels of *FLC* transcript and delayed flowering (Figure 8). These genetic data suggest that the actions of these transcription factors in the regulation of transcription elongation may be more complex than currently understood. Such complex actions have been well illustrated by the contradictory observations with DISF, which acts as a negative elongation factor in vitro but actually facilitates elongation in vivo (Sims et al., 2004). Apparently, DISF is required for transcriptional pausing, but upon phosphorylation of its SPT5 subunit by P-TEFb it can be converted into a positive elongation factor (Sims et al., 2004). DISF interacts with both PAF and P-TEFb, and its dual roles in transcription elongation may explain the opposite roles of *Arabidopsis* PAF-like and P-TEFb–like complexes in the regulation of flowering.

CDKC;2 and its interacting CYCT1;5 partner have an additive role in CaMV infection, based on the more resistant phenotype of the *cdkc;2 cyct1;5* double mutant than the *cdkc;2* and *cyct1;5* single mutants (Figure 1). No such additive role was obvious in the regulation of flowering, since the flowering of the *cdkc;2 cyct1;5* double mutants was similarly delayed as that of the *cdkc;2* single mutants (Figure 8A). In fact, CDKC;2 appeared to be antagonized

by its interacting CYCT1;5 partner in the regulation of *FLC* expression, based on the observation that *FLC* transcript levels were elevated in the *cdkc;2* mutants but not in the *cdkc;2 cyct1;5* double mutants (Figure 8B). It is possible that the role of a CDKC kinase is regulated by its specific CYCT partner and that disruption of a *CYCT1* gene may cause a CDKC to associate with a different CYCT1 to form a complex with an altered function.

The altered phenotypes in the *cdkc* and *cyct1* mutants likely resulted from the inhibited expression of targeted genes important for plant growth and development. In addition, factors affecting transcription elongation can also affect the processing of primary transcripts, such as capping, splicing, and 3′ end formation of mRNA (Sims et al., 2004). Recent genetic studies in *Arabidopsis* indicate that transcripts defective in capping or 3′ end formation are targeted by RDR6-mediated RNA silencing pathways (Gazzani et al., 2004; Herr et al., 2006). Through genetic analysis, we observed that CDKC;2 and RDR6 act cooperatively in the regulation of *Arabidopsis* carpel growth (Figure 8C). CDKC;2 is highly expressed in carpels, and its disruption may lead to the production of truncated or defective transcripts that could be targeted by RDR6-mediated RNA silencing. In the *cdkc;2 rdr6* double mutants, the truncated or defective transcripts may accumulate, leading to abnormal carpel growth through unknown mechanisms.

METHODS

Plant Growth Conditions

Arabidopsis thaliana and *Nicotiana benthamiana* plants were grown in a growth chamber at 22°C with 120 $\mu E \cdot m^{-2} \cdot s^{-1}$ light intensity and a photoperiod of 12 h of light and 12 h of dark.

Identification and Genotyping of Knockout Mutants

The *cdkc;2-1* (SALK_149280), *cdkc;2-2* (SALK_029546), *cyct1;2-1* (SALK_041740), *cyct1;3-1* (SALK_064430), *cyct1;4-1* (SALK_139324), and *cyct1;5-1* (SALK_021004) T-DNA insertion mutants were identified from the Salk *Arabidopsis* T-DNA insertion population (Alonso et al., 2003). *cyct1;3-2* (Flag_396B05) is a T-DNA insertion line obtained from the Institute of Agronomic Research at Versailles, France (Samson et al., 2002). The *cyct1;1-1* (Pst20464) mutant is a *Ds* transposon-tagged line obtained from the RIKEN Genomic Science Center in Yokohama, Japan (Kuromori et al., 2004). Homozygous lines for the mutants were identified by PCR using primers corresponding to sequences flanking the insertion sites (see Supplemental Table 1 online).

Virus Infection

Mechanical inoculation of *Arabidopsis* plants with partially purified CaMV virons was performed as described (Yu et al., 2003b). To inoculate plants by particle bombardment, gold particles (1 μm, 320 μg) were coated with 2 μg of pCa122 plasmid DNA (Kobayashi et al., 2002) and bombarded into *Arabidopsis* plants as described (Xu et al., 2006). Inoculation of *Arabidopsis* plants with TMV-cg or CaLCuV was performed as described (Turnage et al., 2002; Yu et al., 2003a).

DNA and RNA Gel Blot Analyses

Total DNAs from virus-infected leaves were isolated as described (Yu et al., 1999). Total RNA was isolated from frozen plant materials as described (Zheng et al., 2006). DNA and RNA separation, blotting, and hybridization were performed using standard procedures (Sambrook et al., 1989).

Recombinant Protein Production and Kinase Activity Assays

The *CDKC;1* and *CDKC;2* coding sequences were PCR-amplified and cloned into pGEX-4T-1 (Amersham Biosciences) to generate in-frame fusions with the GST tag sequence. The *CYCT1;3* coding sequence was PCR-amplified and cloned into pET-32a (Novagen) to generate His tag sequences. To generate GST fusion proteins containing two repeats of the YSPTSPS heptapeptide, two primers (5′-CGGGATCCTACTCCCC-GACCTCCCCGTCCTACTCCCCGACCTCCCCGTCTTATGCCCCAGAA-TTTCCG-3′ and 5′-CGGAAATTCTGGGGCATAAGACG-3′) were annealed and extended by the Klenow enzyme to form a dsDNA fragment. The fragment was digested with *Bam*HI/*Eco*RI and inserted into pGEX-4T-1. The resulting plasmids were introduced into *Escherichia coli* BL21 cells. Induction of recombinant protein production and purification were performed following the protocols recommended by the manufacturers.

CTD phosphorylation reactions were assembled on ice in a kinase buffer (25 mM Tris-Cl, pH 7.8, 15 mM $MgCl_2$, and 1 mM DTT) containing 2 μg of recombinant GST-tagged CDKC;1 or CDKC;2 protein with or without 2 μg of His-tagged CYCT1;3 recombinant protein. The reactions were initiated by adding 1 μg of GST-CTD substrate protein and 2.5 μCi of [γ-^{32}P]ATP and terminated by the addition of SDS loading buffer after 30 min of incubation at room temperature. The reaction mixtures were separated by 12.5% SDS-PAGE, and CTD phosphorylation was detected by autoradiography.

Yeast Two-Hybrid Assays

Yeast two-hybrid assays were performed with the GAL4 system. The *CDKC;1* and *CDKC;2* coding sequences were amplified and cloned into pBD-GAL4 to generate DNA binding domain fusion partner proteins, and *CYCT1;3*, *CYCT1;4*, and *CYCT1;5* coding sequences were inserted into pAD-GAL4 to form activation domain fusion proteins. All PCR-mediated cloned constructs were verified by sequencing. For interaction analysis, two combinatory constructs were transformed simultaneously into the YRG-2 yeast strain (Stratagene) and tested for $His3^+$, Trp^+, and Leu^+ auxotrophy and LacZ reporter activity (β-galactosidase assay) according to the manufacturer's protocols.

BiFC Assays

DNA sequences for the N-terminal 173–amino acid EYFP (N-YFP) and the C-terminal 64–amino acid (C-YPF) fragments were PCR-amplified and cloned into the plant expression vectors pOCA30 (Chen and Chen, 2002) and pFGC5941 to generate pOCA-N-YFP and pFGC-C-YFP, respectively. The *Arabidopsis CDKC;1* and *CDKC;2* coding sequences were inserted into pOCA-N-YFP to generate the N-terminal in-frame fusions with N-YFP, whereas *CYCT1;3*, *CYCT1;4*, and *CYCT1;5* were introduced into pFGC-C-YFP to form C-terminal in-frame fusions with C-YFP. The resulting clones were verified through sequencing. The plasmids were introduced into *Agrobacterium tumefaciens* (strain GV3101), and infiltration of *N. benthamiana* was performed as described previously (Walter et al., 2004). Confocal microscopy was performed using a Bio-Rad MRC-1024 laser scanning confocal imaging system.

Reporter Gene Assays of the CaMV *35S* Promoter Activity

A *GUS* gene construct driven by the CaMV *35S* promoter was generated by inserting the *GUS* gene into the plant transformation vector pKMB (Mylne and Botella, 1998). This construct was introduced into *Agrobacterium* and then transformed into *Arabidopsis* plants using the floral

dip procedure (Clough and Bent, 1998). Primary transformants were identified by BASTA resistance in soil. GUS activity was measured using 4-methylumbelliferyl-β-D-glucuronide as substrate (Jefferson et al., 1987).

Generation of Transgenic RNAi Lines

To generate *cdkc;2/CDKC;1 RNAi* mutants, an ~300-bp fragment corresponding to the 3′ untranslated sequence of *CDKC;1* was amplified by PCR using primers 5′-atc*ggatccatttaaat*CTGCCCACATATGAATCAT-CAC-3′ (italics are *Bam*HI and *Swa*I sites, and uppercase letters correspond to the sequence of the genes to be amplified; sense primer) and 5′-atc*ggcgcgccactagt*ATCACATTAAATGTAAG-3′ (italics are *Asc*I and *Spe*I sites; antisense primer), and the PCR product was then cloned into appropriate restriction sites of the pFGC5941 RNAi vector (http://www.chromdb.org/fgc5941.html). The resultant construct was transformed into the *cdkc;2-1* mutant background by the *Agrobacterium*-mediated floral dip method. The *cyct1;5/CYCT1;4 RNAi* mutants were generated with the same strategy using an ~350-bp *CYCT1;4* fragment amplified by PCR with the primers 5′-atc*ggcgcgcctctaga*CGAGATTCTTGATGGAAA-CAACTTG-3′ (italics are *Asc*I and *Xba*I sites; sense primer) and 5′-atc-*atttaaatggatcc*GAGACCCTAAATCCTATGGGATGG-3′ (italics are *Swa*I and *Bam*HI sites; antisense primer). The construct was transformed directly into the *cyct1;5-1* mutant background. Seeds from *Agrobacterium*-treated plants were grown directly in soil, and transformants were selected for BASTA resistance. Suppressed expression of the targeted genes was analyzed by RT-PCR or RNA gel blotting.

RT-PCR Analysis

Total RNA was extracted and subjected to reverse transcription with SuperScript III reverse transcriptase (Invitrogen). Two *CDKC;1*-specific primers (5′-CCGGGCTTCACTATTGTCAT-3′ and 5′-GAACCAAGGCAT-CTTGGAAA-3′) were used to amplify a 374-bp product from *CDKC;1*; two *CYCT1;4*-specific primers (5′-AAACCGTGTTCCTGCATCTC-3′ and 5′-GGAAAATGTGCACCTGCTTT-3′) were used to amplify a 327-bp product from *CYCT1;4*; and two *UBQ10*-specific primers (5′-TCA-ATTCTCTCTACCGTGATCAAGATGCA-3′ and 5′-GGTGTCAGAACTCT-CCACCTCAAGAGTA-3′) were used to amplify a 320-bp product from *UBQ10*. PCR conditions were as follows: 94°C for 3 min; followed by 30 cycles at 94°C for 30 s, 56°C for 30 s, and 72°C for 30 s; and a final extension at 72°C for 5 min.

Light and Electron Microscopy

A Nikon SMZ-U stereomicroscope was used to observe siliques and floral structures from wild-type and mutant plants. For scanning electron microscopy, rosette leaves of wild type and mutant plants were cryoprepared with liquid nitrogen. Samples were then examined by NOVA nanoscanning electron microscopy (FEI) operating at 3 kV and ~14-mm working distance.

Promoter–*GUS* Analysis

The ~1.3-kb promoter regions of the *CDKC;1* and *CDKC;2* genes were PCR-amplified from the genomic DNA and cloned into a modified plant expression vector that contains a promoterless *GUS* gene. The promoter–*GUS* constructs were transformed into *Arabidopsis* plants using the *Agrobacterium*-mediated floral dip method. Histochemical staining of GUS activity was performed as described previously (Jefferson et al., 1987).

Accession Numbers

Arabidopsis Genome Initiative locus identifiers for the genes mentioned in this article are as follows: *CDKC;1* (At5g10270), *CDKC;2* (At5g64960), *CYCT1;1* (At1g35440), *CYCT1;2* (At4g19560), *CYCT1;3* (At1g27630), *CYCT1;4* (At4g19600), *CYCT1;5* (At5g45190), *FLC* (At5g10140), *NRPB1* (At4g35800), and *UBQ10* (At4g05320).

Supplemental Data

The following materials are available in the online version of this article.

Supplemental Table 1. PCR Primers Used in Knockout Mutant Screening.

Supplemental Figure 1. Sequence Comparison of *Arabidopsis* CDKC and CYCT1 Proteins.

Supplemental Figure 2. Diagram of *Arabidopsis* Genes and T-DNA Insertion or Transposon-Tagging Mutants.

Supplemental Figure 3. Genetic Complementation of the *cyct1;5* Mutant.

Supplemental Figure 4. RT-PCR Analysis of *CDKC;1* and *CYCT1;4* Transcripts from RNAi Plants.

ACKNOWLEDGMENTS

We thank Thomas Hohn (University of Basel, Basel, Switzerland) and Seiji Tsuge (Kyoto Prefectural University, Kyoto, Japan) for kindly providing the plasmid pCa122 and Dominique Niki Robertson (North Carolina State University, Raleigh) for CaLCuV plasmids. We also thank Chang-Deng Hu (Purdue University, West Lafayette, IN) for providing EYFP plasmids, Scott Poethig (University of Pennsylvania, Philadelphia) for *rdr6-11* seeds, and the Arabidopsis Biological Resource Center at Ohio State University, the Institute of Agronomic Research (Versailles, France), and the RIKEN Genomic Science Center (Yokohama, Japan) for T-DNA insertion or Ds-tagged mutants. We are grateful to Debby Sherman for help with scanning electron microscopy. This is Journal Paper 2007-18103 of the Purdue University Agricultural Research Program.

Received February 24, 2007; revised March 20, 2007; accepted April 5, 2007; published April 27, 2007.

REFERENCES

Adamson, T.E., Shutt, D.C., and Price, D.H. (2005). Functional coupling of cleavage and polyadenylation with transcription of mRNA. J. Biol. Chem. **280:** 32262–32271.

Akoulitchev, S., Chuikov, S., and Reinberg, D. (2000). TFIIH is negatively regulated by cdk8-containing mediator complexes. Nature **407:** 102–106.

Alonso, J.M., et al. (2003). Genome-wide insertional mutagenesis of *Arabidopsis thaliana.* Science **301:** 653–657.

Barroco, R.M., De Veylder, L., Magyar, Z., Engler, G., Inze, D., and Mironov, V. (2003). Novel complexes of cyclin-dependent kinases and a cyclin-like protein from *Arabidopsis thaliana* with a function unrelated to cell division. Cell. Mol. Life Sci. **60:** 401–412.

Brady, J., and Kashanchi, F. (2005). Tat gets the ''green'' light on transcription initiation. Retrovirology **2:** 69.

Chen, C., and Chen, Z. (2002). Potentiation of developmentally regulated plant defense response by AtWRKY18, a pathogen-induced Arabidopsis transcription factor. Plant Physiol. **129:** 706–716.

Clough, S.J., and Bent, A.F. (1998). Floral dip: A simplified method for *Agrobacterium*-mediated transformation of *Arabidopsis thaliana.* Plant J. **16:** 735–743.

Dietrich, M.A., Prenger, J.P., and Guilfoyle, T.J. (1990). Analysis of the genes encoding the largest subunit of RNA polymerase II in *Arabidopsis* and soybean. Plant Mol. Biol. **15:** 207–223.

Flint, J., and Shenk, T. (1997). Viral transactivating proteins. Annu. Rev. Genet. **31:** 177–212.

Fulop, K., Pettko-Szandtner, A., Magyar, Z., Miskolczi, P., Kondorosi, E., Dudits, D., and Bako, L. (2005). The Medicago CDKC;1-CYCLINT;1 kinase complex phosphorylates the carboxy-terminal domain of RNA polymerase II and promotes transcription. Plant J. **42:** 810–820.

Gazzani, S., Lawrenson, T., Woodward, C., Headon, D., and Sablowski, R. (2004). A link between mRNA turnover and RNA interference in *Arabidopsis.* Science **306:** 1046–1048.

Hanley-Bowdoin, L., Settlage, S.B., Orozco, B.M., Nagar, S., and Robertson, D. (2000). Geminiviruses: Models for plant DNA replication, transcription, and cell cycle regulation. Crit. Rev. Biochem. Mol. Biol. **35:** 105–140.

He, Y., Doyle, M.R., and Amasino, R.M. (2004). PAF1-complex-mediated histone methylation of FLOWERING LOCUS C chromatin is required for the vernalization-responsive, winter-annual habit in *Arabidopsis.* Genes Dev. **18:** 2774–2784.

Herr, A.J., Molnar, A., Jones, A., and Baulcombe, D.C. (2006). Defective RNA processing enhances RNA silencing and influences flowering of *Arabidopsis.* Proc. Natl. Acad. Sci. USA **103:** 14994–15001.

Hull, R. (2002). Matthews' Plant Virology. (San Diego, CA: Academic Press).

Ishikawa, M., Obata, F., Kumagai, T., and Ohno, T. (1991). Isolation of mutants of *Arabidopsis thaliana* in which accumulation of tobacco mosaic virus coat protein is reduced to low levels. Mol. Gen. Genet. **230:** 33–38.

Jefferson, R.A., Kavanagh, T.A., and Bevan, M.W. (1987). GUS fusions: Beta-glucuronidase as a sensitive and versatile gene fusion marker in higher plants. EMBO J. **6:** 3901–3907.

Joubes, J., Lemaire-Chamley, M., Delmas, F., Walter, J., Hernould, M., Mouras, A., Raymond, P., and Chevalier, C. (2001). A new C-type cyclin-dependent kinase from tomato expressed in dividing tissues does not interact with mitotic and G1 cyclins. Plant Physiol. **126:** 1403–1415.

Kiss-Laszlo, Z., and Hohn, T. (1996). Pararetro- and retrovirus RNA: Splicing and the control of nuclear export. Trends Microbiol. **4:** 480–485.

Kobayashi, K., Tsuge, S., Stavolone, L., and Hohn, T. (2002). The cauliflower mosaic virus virion-associated protein is dispensable for viral replication in single cells. J. Virol. **76:** 9457–9464.

Koiwa, H., et al. (2002). C-terminal domain phosphatase-like family members (AtCPLs) differentially regulate *Arabidopsis thaliana* abiotic stress signaling, growth, and development. Proc. Natl. Acad. Sci. USA **99:** 10893–10898.

Koiwa, H., Hausmann, S., Bang, W.Y., Ueda, A., Kondo, N., Hiraguri, A., Fukuhara, T., Bahk, J.D., Yun, D.J., Bressan, R.A., Hasegawa, P.M., and Shuman, S. (2004). *Arabidopsis* C-terminal domain phosphatase-like 1 and 2 are essential Ser-5-specific C-terminal domain phosphatases. Proc. Natl. Acad. Sci. USA **101:** 14539–14544.

Krogan, N.J., Dover, J., Wood, A., Schneider, J., Heidt, J., Boateng, M.A., Dean, K., Ryan, O.W., Golshani, A., Johnston, M., Greenblatt, J.F., and Shilatifard, A. (2003). The Paf1 complex is required for histone H3 methylation by COMPASS and Dot1p: Linking transcriptional elongation to histone methylation. Mol. Cell **11:** 721–729.

Kuromori, T., Hirayama, T., Kiyosue, Y., Takabe, H., Mizukado, S., Sakurai, T., Akiyama, K., Kamiya, A., Ito, T., and Shinozaki, K. (2004). A collection of 11 800 single-copy Ds transposon insertion lines in *Arabidopsis.* Plant J. **37:** 897–905.

Luo, Z., and Chen, Z. (2007). Improperly terminated, unpolyadenylated mRNA of sense transgenes is targeted by RDR6-mediated RNA silencing in *Arabidopsis.* Plant Cell **19:** 943–958.

Mancebo, H.S., Lee, G., Flygare, J., Tomassini, J., Luu, P., Zhu, Y., Peng, J., Blau, C., Hazuda, D., Price, D., and Flores, O. (1997). P-TEFb kinase is required for HIV Tat transcriptional activation in vivo and in vitro. Genes Dev. **11:** 2633–2644.

Marshall, N.F., and Price, D.H. (1995). Purification of P-TEFb, a transcription factor required for the transition into productive elongation. J. Biol. Chem. **270:** 12335–12338.

Menges, M., de Jager, S.M., Gruissem, W., and Murray, J.A. (2005). Global analysis of the core cell cycle regulators of *Arabidopsis* identifies novel genes, reveals multiple and highly specific profiles of expression and provides a coherent model for plant cell cycle control. Plant J. **41:** 546–566.

Mylne, J., and Botella, J.R. (1998). Binary vectors for sense and antisense expression of *Arabidopsis* ESTs. Plant Mol. Biol. Rep. **16:** 257–262.

Ni, Z., Schwartz, B.E., Werner, J., Suarez, J.R., and Lis, J.T. (2004). Coordination of transcription, RNA processing, and surveillance by P-TEFb kinase on heat shock genes. Mol. Cell **13:** 55–65.

Nigg, E.A. (1996). Cyclin-dependent kinase 7: At the cross-roads of transcription, DNA repair and cell cycle control? Curr. Opin. Cell Biol. **8:** 312–317.

Odell, J.T., Nagy, F., and Chua, N.H. (1985). Identification of DNA sequences required for activity of the cauliflower mosaic virus 35S promoter. Nature **313:** 810–812.

Oh, S., Zhang, H., Ludwig, P., and van Nocker, S. (2004). A mechanism related to the yeast transcriptional regulator Paf1c is required for expression of the *Arabidopsis* FLC/MAF MADS box gene family. Plant Cell **16:** 2940–2953.

Peng, J., Zhu, Y., Milton, J.T., and Price, D.H. (1998). Identification of multiple cyclin subunits of human P-TEFb. Genes Dev. **12:** 755–762.

Peragine, A., Yoshikawa, M., Wu, G., Albrecht, H.L., and Poethig, R.S. (2004). SGS3 and SGS2/SDE1/RDR6 are required for juvenile development and the production of trans-acting siRNAs in *Arabidopsis.* Genes Dev. **18:** 2368–2379.

Pinhero, R., Liaw, P., Bertens, K., and Yankulov, K. (2004). Three cyclin-dependent kinases preferentially phosphorylate different parts of the C-terminal domain of the large subunit of RNA polymerase II. Eur. J. Biochem. **271:** 1004–1014.

Qiu, H., Hu, C., Wong, C.M., and Hinnebusch, A.G. (2006). The Spt4p subunit of yeast DSIF stimulates association of the Paf1 complex with elongating RNA polymerase II. Mol. Cell. Biol. **26:** 3135–3148.

Sambrook, J., Fritsch, E.F., and Maniatis, T. (1989). Molecular Cloning: A Laboratory Manual. (Cold Spring Harbor, NY: Cold Spring Harbor Laboratory Press).

Samson, F., Brunaud, V., Balzergue, S., Dubreucq, B., Lepiniec, L., Pelletier, G., Caboche, M., and Lecharny, A. (2002). FLAGdb/FST: A database of mapped flanking insertion sites (FSTs) of *Arabidopsis thaliana* T-DNA transformants. Nucleic Acids Res. **30:** 94–97.

Shepherd, R.J., Bruening, G.E., and Wakeman, R.J. (1970). Double-stranded DNA from cauliflower mosaic virus. Virology **41:** 339–347.

Shepherd, R.J., Wakeman, R.J., and Romanko, R.R. (1968). DNA in cauliflower mosaic virus. Virology **36:** 150–152.

Shimotohno, A., Matsubayashi, S., Yamaguchi, M., Uchimiya, H., and Umeda, M. (2003). Differential phosphorylation activities of CDK-activating kinases in *Arabidopsis thaliana.* FEBS Lett. **534:** 69–74.

Sims, R.J., III, Belotserkovskaya, R., and Reinberg, D. (2004). Elongation by RNA polymerase II: The short and long of it. Genes Dev. **18:** 2437–2468.

Stavolone, L., Villani, M.E., Leclerc, D., and Hohn, T. (2005). A coiled-coil interaction mediates cauliflower mosaic virus cell-to-cell movement. Proc. Natl. Acad. Sci. USA **102:** 6219–6224.

Turnage, M.A., Muangsan, N., Peele, C.G., and Robertson, D. (2002). Geminivirus-based vectors for gene silencing in *Arabidopsis.* Plant J. **30:** 107–114.

Walter, M., Chaban, C., Schutze, K., Batistic, O., Weckermann, K., Nake, C., Blazevic, D., Grefen, C., Schumacher, K., Oecking, C., Harter, K., and Kudla, J. (2004). Visualization of protein interactions in living plant cells using bimolecular fluorescence complementation. Plant J. **40:** 428–438.

Wang, G., Kong, H., Sun, Y., Zhang, X., Zhang, W., Altman, N., DePamphilis, C.W., and Ma, H. (2004). Genome-wide analysis of the cyclin family in Arabidopsis and comparative phylogenetic analysis of plant cyclin-like proteins. Plant Physiol. **135:** 1084–1099.

Wang, W., and Chen, X. (2004). HUA ENHANCER3 reveals a role for a cyclin-dependent protein kinase in the specification of floral organ identity in *Arabidopsis.* Development **131:** 3147–3156.

Xu, X., Chen, C., Fan, B., and Chen, Z. (2006). Physical and functional interactions between pathogen-induced *Arabidopsis* WRKY18, WRKY40, and WRKY60 transcription factors. Plant Cell **18:** 1310–1326.

Yu, D., Fan, B., MacFarlane, S.A., and Chen, Z. (2003a). Analysis of the involvement of an inducible *Arabidopsis* RNA-dependent RNA polymerase in antiviral defense. Mol. Plant Microbe Interact. **16:** 206–216.

Yu, D., Xie, Z., Chen, C., Fan, B., and Chen, Z. (1999). Expression of tobacco class II catalase gene activates the endogenous homologous gene and is associated with disease resistance in transgenic potato plants. Plant Mol. Biol. **39:** 477–488.

Yu, W., Murfett, J., and Schoelz, J.E. (2003b). Differential induction of symptoms in *Arabidopsis* by P6 of cauliflower mosaic virus. Mol. Plant Microbe Interact. **16:** 35–42.

Zhang, H., and van Nocker, S. (2002). The VERNALIZATION INDEPENDENCE 4 gene encodes a novel regulator of FLOWERING LOCUS C. Plant J. **31:** 663–673.

Zheng, Z., Qamar, S.A., Chen, Z., and Mengiste, T. (2006). *Arabidopsis* WRKY33 transcription factor is required for resistance to necrotrophic fungal pathogens. Plant J. **48:** 592–605.

Zhou, M., Lu, H., Park, H., Wilson-Chiru, J., Linton, R., and Brady, J.N. (2006). Tax interacts with P-TEFb in a novel manner to stimulate human T-lymphotropic virus type 1 transcription. J. Virol. **80:** 4781–4791.